Shahrood University of Technology
Iranian Society of Mining Engineering (IRSME)
Journal of Mining and Environment (JME)
journal homepage: www.jme.shahroodut.ac.ir
THOMSON REUTERS
Vol. 11, No. 3, 2020, 855-864.
DOI: 10.22044/jme.2020.9581.1872

Behavior of a Tunnel and its Neighboring Joint with and without Presence of Rock Bolt under Biaxial Loads; Particle Flow Code Approach

V. Sarfarazi*

Department of Mining Engineering, Hamedan University of Technology, Hamedan, Iran

Received 18 April 2020; received in revised form 28 May 2020; accepted 24 May 2020

Keywords

PFC2D

Tunnel

Joint

Rock bolt

Tensile crack

Abstract

In this work, the interaction between the semi-circular space and the neighboring joint with and without the presence of rock bolts was investigated using the particle flow code (PFC) approach. For this purpose, firstly, the calibration of PFC was performed using both the Brazilian experimental test and the uniaxial compression test. Secondly, a numerical model with the dimension of 100 mm * 100 mm was prepared. A semi-circular space with a radius of 25 mm was situated below the model. A joint with a length of 40 mm was situated above the space. The joint opening was 2 mm. The joint angles related to the horizontal direction were 0°, 15°, 30°, 45°, 60°, and 75°. Totally, 6 different configurations of the semi-circular space and neighboring joint were prepared. These models were tested with and without the presence of vertical rock bolts by the biaxial test. The rock bolt length was 50 mm. The value of the lateral force was fixed at 2 MPa. An axial force was applied to the model till the final failure occurred. The results obtained showed that the presence of rock bolts changed the failure pattern of the numerical model. In the absence of rock bolts, two tensile wing cracks initiated from the joint tip and propagated diagonally till coalescence from the model boundary. Also several shear bands were initiated in the left and right sides of the tunnel. In the presence of rock bolts, several shear bands were initiated in the left and right sides of the tunnel. The compressive strength with the presence of rock bolts was more than that without the presence of rock bolts. The failure stress had a minimum value when the joint angle was 45°.

1. Introduction

A tunnel excavation will cause the re-adjustment of the existing stress fields in the surrounding rock masses. Rock bolts have been widely used to reinforce the surrounding rock mass in a tunnel engineering. A proper design of rock bolts, which depends on the full understanding of the mechanism and effectiveness of rock bolts, is very important to the reinforcement, stabilization, and safety construction of rock tunnels [1–3]. Meanwhile, there are lots of uncertainties in the rock tunnels. The uncertainties are critical to the design and safe construction due to the complexity of rock mass [4]. The reliability analysis is a widely developed method used to determine the uncertainty in an engineering system [5]. The stresses and displacements around a tunnel with and without the presence of rock bolts is an important problem considering the uncertainty in the tunnel engineering.

Various analytical, experimental, and numerical methods have been developed to analyze and understand the mechanism of rock bolts in the tunnels based on different assumptions and conditions. The analytical models are capable of defining the stresses and the deformations, and have been widely used due to the computational simplicity [6, 7]. Hoek and Brown (1980) have presented analytical solutions of tunnels with rock bolts [8]. Brown et al. (1983) have proposed an analytical solution based on the elastic-brittle-plastic material behavior and Hoek-Brown yield criterion [9]. Li and Stillborg (1999) have

✉ *Corresponding author: sarfarazi@hut.ac.ir (V. Sarfarazi).*

developed three analytical models for rock bolts based on the mechanical coupling at various interfaces of the rock bolts, the grout medium, and the rock mass [2]. Cai et al. (2004) have described the interaction mechanism between the rock bolts and rock mass, proposing an analytical model to analyze the supporting behavior of rock bolts in tunnels [10]. Guan et al. (2007) have considered the interaction relationship between rock bolts and rock mass, proposing a framework to analyze the elasto-plastic ground response of the tunnels with rock bolts [11]. Oreste (2008) has proposed a calculation procedure to determine the stress and strain state of rock mass in a tunnel with rock bolts [12]. Indraratna and Kaiser (1990) have extended the general solutions based on the Mohr–Coulomb criterion, and have developed an elastic-brittle plastic model [13]. Fahimifar and Soroush (2005) have presented a new approach based on a non-linear strength criterion for rock mass and the brittle and strain softening stress–strain behavior models [14]. Carranza-Torres (2009) have analyzed the mechanical contribution of rock bolt reinforcement based on the elasto-plastic model, proving that rock bolts can also have a critical effect on controlling the extent of the plastic failure zone and the convergences of the tunnel [15]. Bobet and Einstein (2011) have analyzed the reinforcement mechanism of different types of bolts, proposing an analytical solution for a circular tunnel with rock bolts based on the coupling analysis [16]. The above models have been used in the design of rock bolts and the stability analysis of tunnels. However, these models did not deal with the uncertainties in the variables such as the rock mass strength and the parameters of the rock bolts. The reliability method has been developed for the stability analysis of tunnels to consider the uncertainty [5, 17–21]. Hoek (1998) has applied the reliability method to the stability analysis of circular tunnels through integrating the analytical solutions and Monte Carlo simulation [22]. Li and Low (2010) have analyzed the stability of the circular tunnels subjected to hydrostatic stress by combining an analytical solution with the first-order reliability method (FORM) [18]. Zhang and Goh (2012) have estimated the stability of underground rock cavern using the reliability method [23].

In this work, the behavior of a tunnel and the neighboring joint with and without the presence of rock bolts was studied using the Particle Flow Code (PFC).

The aim of this work was to analyses the effect of the presence of rock bolts on the failure pattern, stress concentration at the tip of the joint, and the vertical displacement at the tunnel roof.

2. Numerical simulation

2.1. Bonded particle model and particle flow code in two dimensions (PFC2D)

PFC2D is a distinct element code that represents the materials as an assembly of rigid particles that can move independently from one another and interact only at contacts (Itasca 1999 version 3.1 [24]; Potyondy and Cundall, 2004 [25]). The movements and interaction forces of particles are calculated using a central finite difference method as applied in DEM. For the models of the contacts, both the linear and non-linear contact models with frictional sliding can be used. The linear contact model used in this work provides an elastic relationship between the relative displacements and the contact forces of particles. In order to generate a parallel-bonded particle model for PFC2D, using the routines provided (Itasca 1999, version 3.1), the following micro-properties should be defined: ball-to-ball contact modulus, stiffness ratio kn over ks, ball friction coefficient, parallel normal bond strength, parallel shear bond strength, ratio of standard deviation to mean of bond strength both in the normal and shear directions, minimum ball radius, parallel-bond radius multiplier, parallel-bond modulus, and parallel-bond stiffness ratio. In order to establish the appropriate micro-properties to be used for the particle assembly, it is necessary to conduct a calibration procedure. The particle contact properties and bonding characteristics cannot be determined directly from the tests performed on the laboratory model samples. The material properties determined by laboratory experimentation are macro-mechanical in nature because they reflect the continuum behavior. An inverse modelling procedure was used to determine the appropriate micro-mechanical properties of the numerical models from the macro-mechanical properties determined in the laboratory tests. The trial-and-error approach is one of the methods used to relate these two sets of material properties (Itasca 1999 [24]). It involves assumption of the micro-mechanical property values and comparison of the strength and deformation characteristics of the numerical models with those of the laboratory samples. The micro-mechanical property values that give a simulated macroscopic response close to that of the laboratory tests are then adopted for the discontinuous jointed blocks. The limitations of DEM are (Donze et al. 2009 [26]): (a) Fracture is closely related to the size of elements, and that is

so-called the size effect. (b) Cross effect exists due to the difference between the size and shape of the elements with real grains. (c) In order to establish the relationship between the local and macroscopic constitutive laws, the data obtained from the classical geo-mechanical tests, which may be impractical, is used.

2.2. Preparing and calibrating numerical model

The standard process of generating a PFC2D assembly to represent a test model, used in this work, has been described in detail by Potyondy and Cundall [22]. This process involves particle generation, packing the particles, isotropic stress installation (stress initialization), floating particle (floater) elimination, and bond installation. A gravity effect was not required to be considered as the specimens were small, and the gravity-induced stress gradient had a negligible effect on the macroscopic behavior. The uniaxial compressive strength and Brazilian tests were carried out to calibrate the properties of particles and parallel bonds in the bonded particle model. Adopting the micro-properties listed in Table 1 and the standard calibration procedures (Potyondy and Cundall [22]), a calibrated PFC particle assembly was created. Figure 1 shows the numerical compression test results. The red line and black line show the shear crack and the tensile cracks, respectively. As it can be seen, the tensile cracks develop within the model. This is in accordance to the typical failure pattern occurring in the experimental test.

Figures. 2a and 2b show the experimental Brazilian test and the numerical simulation, respectively. The results obtained show a well-matching between the experimental test and the numerical simulation. Table 2 shows the results of a comparison between the mechanical properties rendered by the experimental test and the numerical simulation. The results show a well-matching between the experimental test and the numerical simulation.

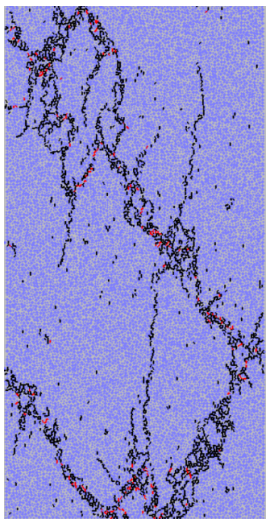

Figure 1. Numerical compression test results.

Table 1. Micro-properties used to represent the intact rocks.

Parameter	Value	Parameter	Value
Type of particle	disc	Parallel bond radius multiplier	1
Density	3000	Young modulus of parallel bond (GPa)	40
Minimum radius	0.27	Parallel bond stiffness ratio	1.7
Size ratio	1.56	Particle friction coefficient	0.4
Porosity ratio	0.08	Parallel bond normal strength, mean (MPa)	10
Damping coefficient	0.7	Parallel bond normal strength, SD (MPa)	2
Contact young modulus (GPa)	40	Parallel bond shear strength, mean (MPa)	10
Stiffness ratio	1.7	Parallel bond shear strength, SD (MPa)	2

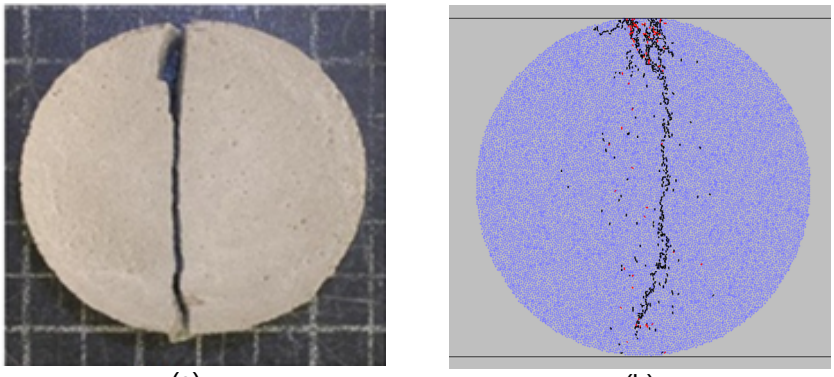

(a) (b)

Figure 2. Failure pattern in a) physical sample, b) PFC2D model.

Table 2. Mechanical properties in numerical models.

Parameter	Numerical output	Experimental result
Uniaxial compressive strength (MPa)	7.4	7.2
Young modulus (GPa)	9.3	9.1
Tensile strength (MPa)	1.4	1.3

2.3 Model preparation using PFC

After calibration of PFC2D, a biaxial test was simulated by creating a rectangular model in PFC2D (using the calibrated micro-parameters) (Figure 3). The PFC specimen had the dimension of 10 cm * 10 cm. A semi-circular tunnel with a diameter of 5 cm was situated below the model (Figure 3). Two narrow clumps exist below the model to transmit the axial force into the model. A joint with a length of 40 mm was situated above the tunnel (Figure 3). The joint angles related to the horizontal direction were 0˚, 15˚, 30˚, 45˚, 60˚, and 75˚ (Figure 3). A measuring circle with a diameter of 1 cm exists at the tip of the joint to measure the stress concentration (Figure 3a). This measuring circle was installed in all the numerical models. Four balls with the different ball identifications of 1239, 4365, 3009, and 7908 were selected at the tunnel roof to measure the mean vertical displacement (Figure 3a). These balls were chosen in all the numerical models. Totally, 6 various configurations of the tunnel and the neighboring joint were prepared. These models were tested without the presence of rock bolts (Figure 3) and with the presence of rock bolts (Figure 4) under the biaxial test. The rock bolt simulated by clump particle had a green color (Figure 4) and its length was 6 cm. This bolt was situated vertically in the model. These models were loaded biaxially. The confining pressure was 1 MPa. The compressive force was registered by taking the reaction forces on the upper wall.

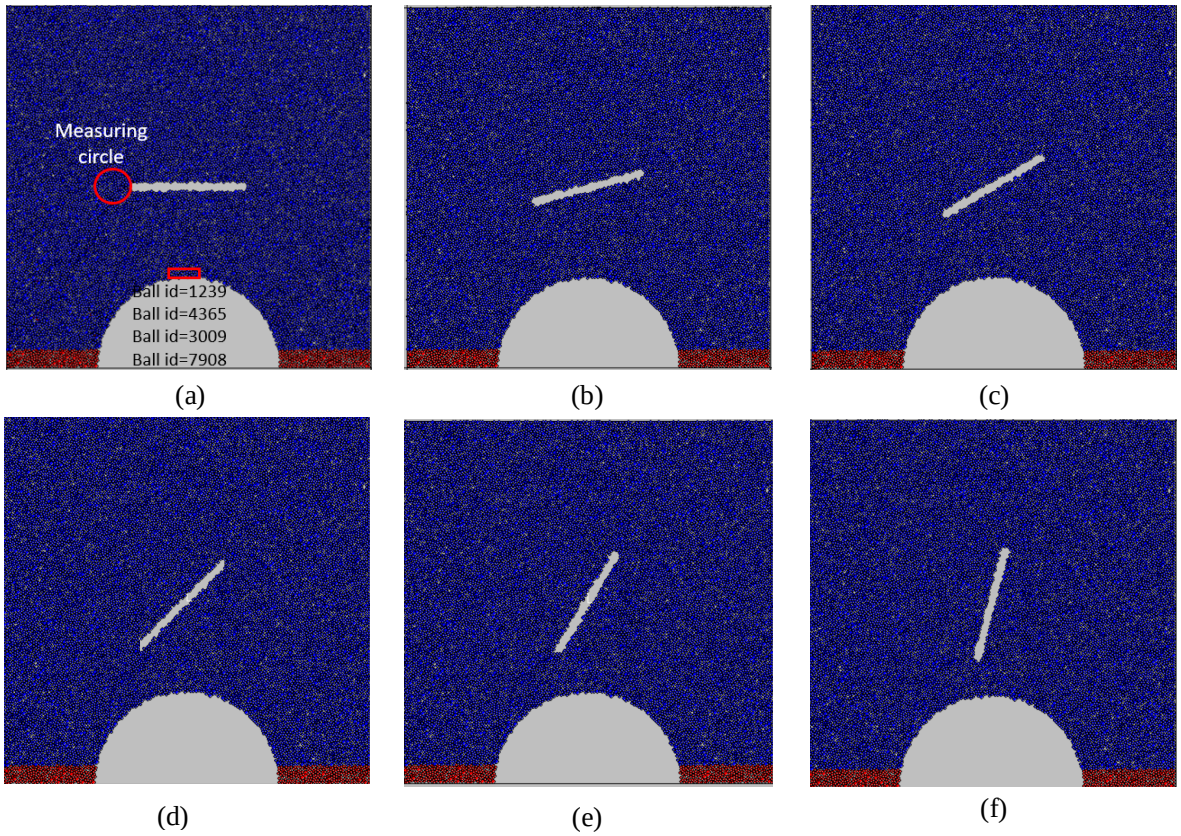

Figure 3. Semi-circular tunnel and neighboring joint with angles of; a) 0˚, b) 15˚, c) 30˚, d) 45˚, e) 60˚, and f) 75˚.

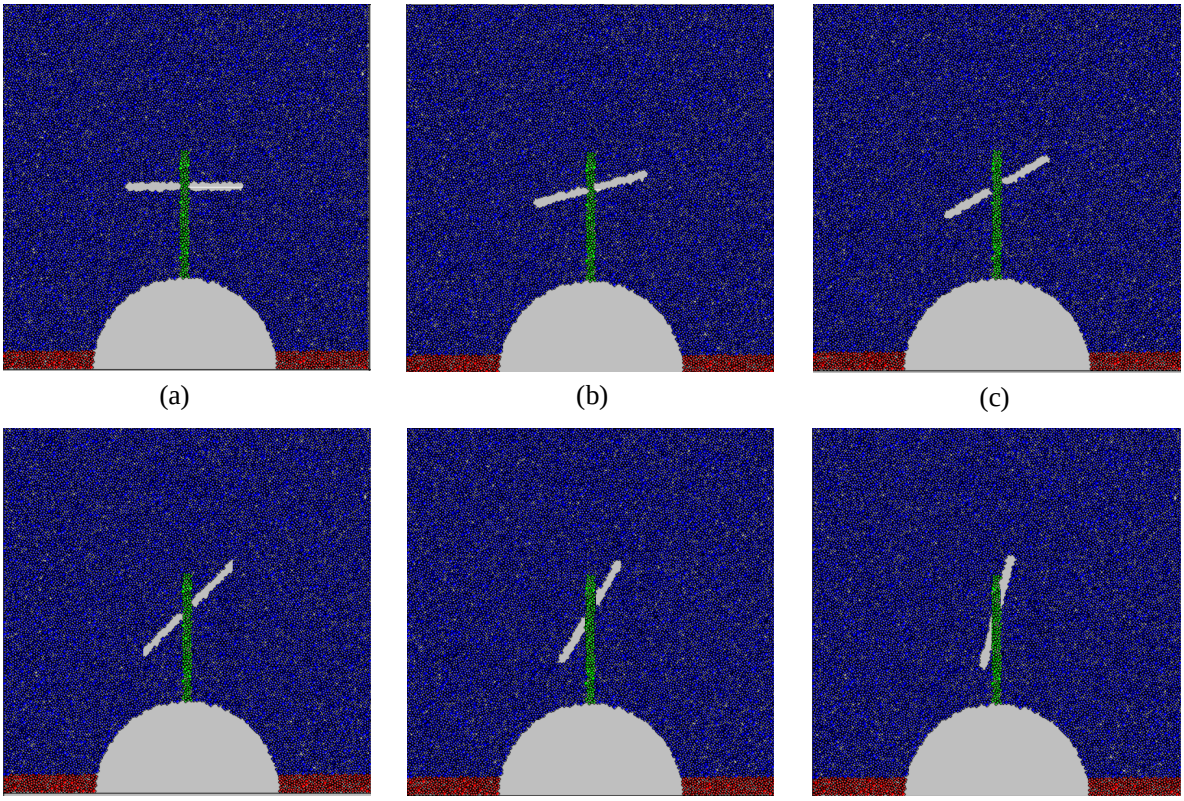

Figure 4. Semi-circular tunnel and neighboring joint with angles of; a) 0°, b) 15°, c) 30°, d) 45°, e) 60°, and f) 75°.

3. Numerical results

3.1. Effect of joint angle on failure pattern of numerical model (without presence of rock bolts)

Figure 5 shows the effect of joint angle on the failure pattern of the numerical model without the presence of rock bolt. The black line and the red line represent the tensile crack and shear crack, respectively.

a. When the joint angle was 0° (Figure 5a), two tensile wing cracks initiated from the joint tip and propagated diagonally till coalescence from the model boundary. Also several shear bands were initiated in the left and right sides of the tunnel.

b. When the joint angle was 15° (Figure 5b), one tensile wing crack initiated from the joint tip and propagated diagonally till coalescence from the model boundary. Also several shear bands were initiated in the left and right sides of the tunnel.

c. When the joint angle was 30° (Figure 5c), one tensile wing crack initiated from the joint tip and propagated diagonally till coalescence from the model boundary. Also several shear bands were initiated in the left and right sides of the tunnel.

d. When the joint angle was 45° (Figure 5d), two tensile wing cracks initiated from the joint tip and propagated diagonally till coalescence from the model boundary. Also several shear bands were initiated in the left and right sides of the tunnel.

e. When the joint angle was 60° (Figure 5e), several shear bands were initiated in the left and right sides of the tunnel.

f. When the joint angle was 75° (Figure 5f), several shear bands were initiated in the left and right sides of the tunnel.

It is clear that in the absence of rock bolt, when the joint angle is less than 45°, two tensile wing cracks initiate from the joint tip and propagate diagonally till coalescence from the model boundary. In these configurations, a wedge block formed in the top of the tunnel roof. When the joint angle was more than 45°, several shear bands were initiated in the left and right sides of the tunnel. In this configuration, the pillars failed heavily.

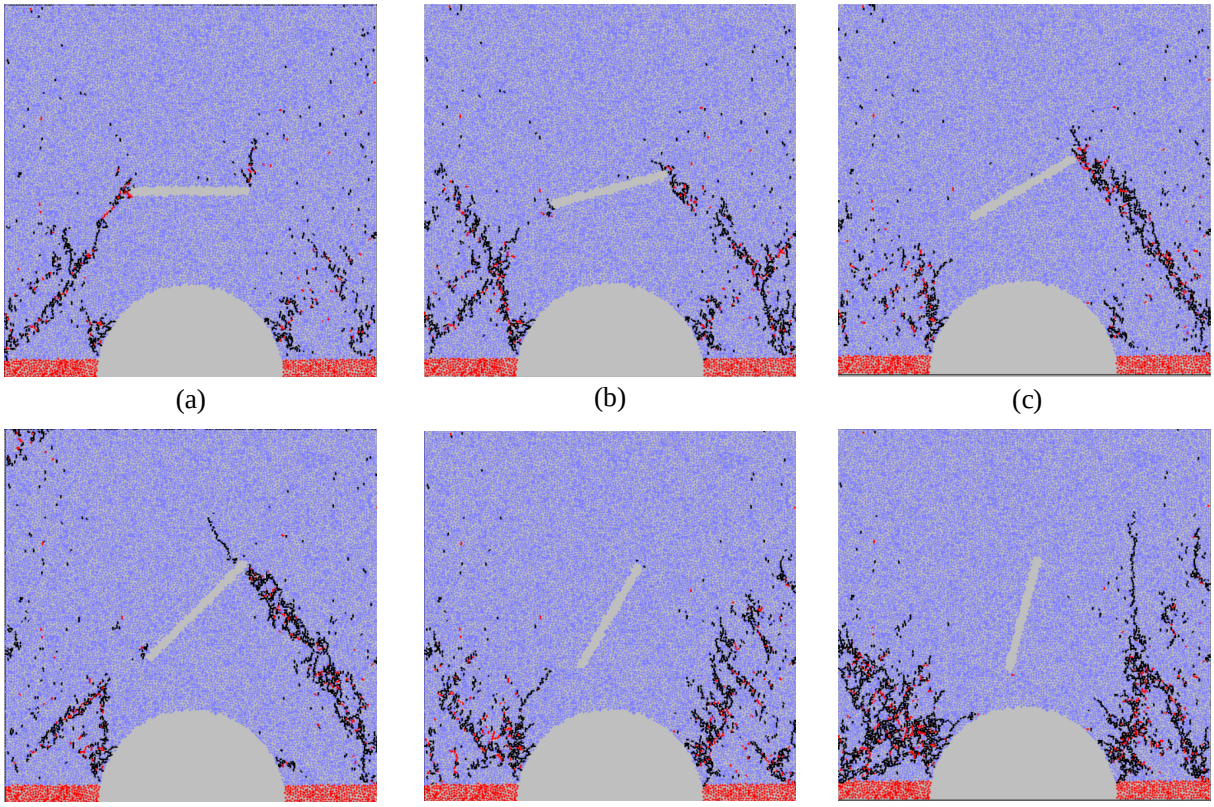

Figure 5. Semi-circular tunnel and neighboring joint with angles of a) 0˚, b) 15˚, c) 30˚, d) 45˚, e) 60˚, and f) 75.

3.2. Effect of joint angle on failure pattern of numerical model (with presence of rock bolt)

Figure 6 shows the effect of joint angle on the failure pattern of the numerical model with the presence of rock bolt. The black line and the red line represent the tensile crack and the shear crack, respectively.

a. When the joint angle was 0˚ (Figure 6a), several shear bands were initiated in the left and right sides of the tunnel.

b. When the joint angle was 15˚ (Figure 6b), several shear bands were initiated in the left and right sides of the tunnel.

c. When the joint angle was 30˚ (Figure 6c), several shear bands were initiated in the left and right sides of the tunnel.

d. When the joint angle was 45˚ (Figure 6d), several shear bands were initiated in the left and right sides of the tunnel.

e. When the joint angle was 60˚ (Figure 6e), several shear bands were initiated in the left and right sides of the tunnel.

f. When the joint angle was 75˚ (Figure 6f), several shear bands were initiated in the left and right sides of the tunnel.

By a comparison between Figs. 3 and 4, it could be concluded that the wing cracks disappeared from the joint tips in the presence of rock bolts. Also the failure extension in the supported tunnel was less than that in the unsupported tunnel.

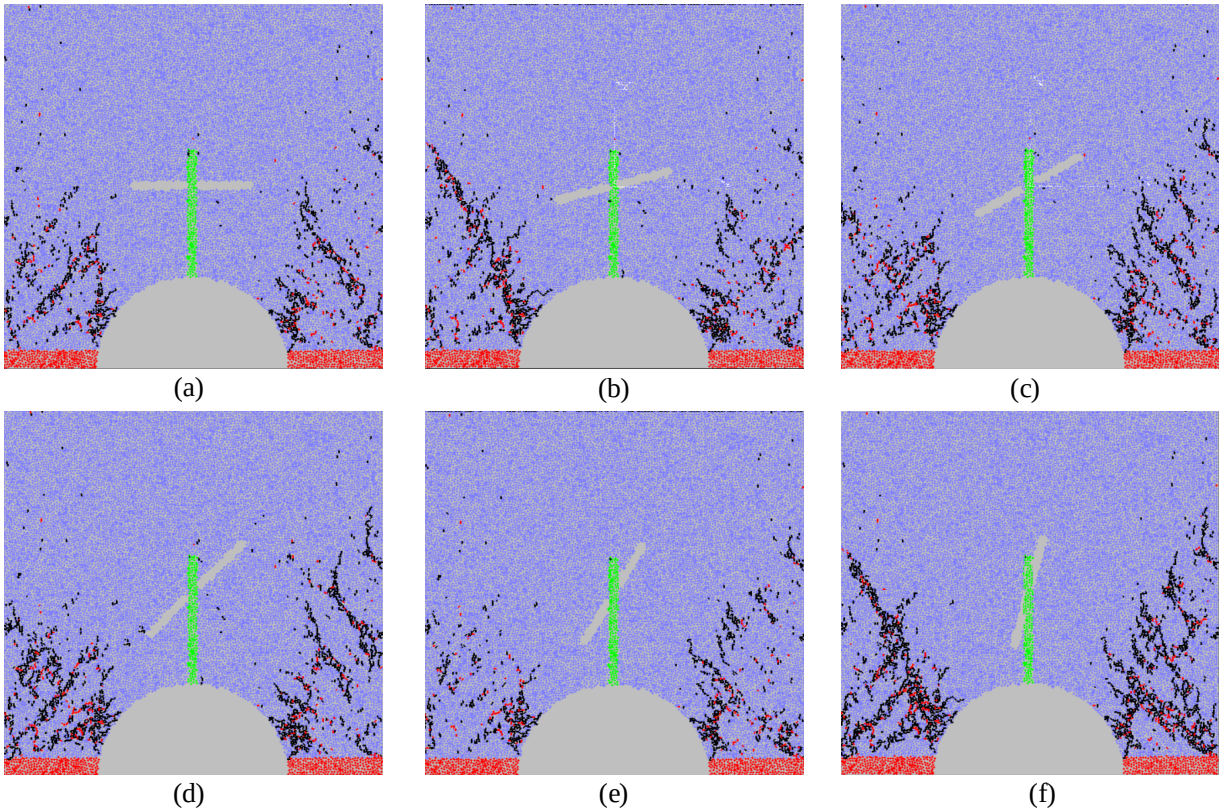

Figure 6. Semi-circular tunnel and neighboring joint with angles of; a) 0˚, b) 15˚, c) 30˚, d) 45˚, e) 60˚, and f) 75˚.

3.3. Effect of joint angle on stress concentration at tip of joint with and without presence of rock bolt when vertical displacement of loading wall is 0.01 mm

Figure 7 shows the effect of joint angle on the stress concentration at the tip of the joint with and without the presence of rock bolt when vertical displacement of loading wall was 0.01 mm. The stress concentration at the tip of the joint without the presence of rock bolt is more than that with the presence of rock bolt. Also the stress concentration at the tip of the joint had a maximum value when the joint angle was 45˚.

3.4. Effect of joint angle on vertical displacement of tunnel roof with and without presence of rock bolt when vertical displacement of loading wall is 0.01 mm

Figure 8 shows the effect of the joint angle on the vertical displacement of the tunnel roof with and without the presence of rock bolt when the vertical displacement of loading wall was 0.01 mm. The vertical displacement of tunnel roof without the presence of rock bolt was more than that with the presence of rock bolt. Also the vertical displacement of the tunnel roof had a maximum value when the joint angle was 45˚.

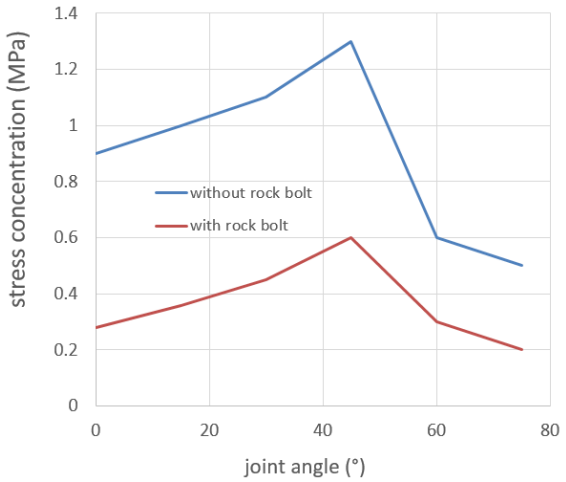

Figure 7. Effect of joint angle on the stress concentration at the tip of the joint with and without the presence of rock bolt when vertical displacement of loading wall was 0.01 mm.

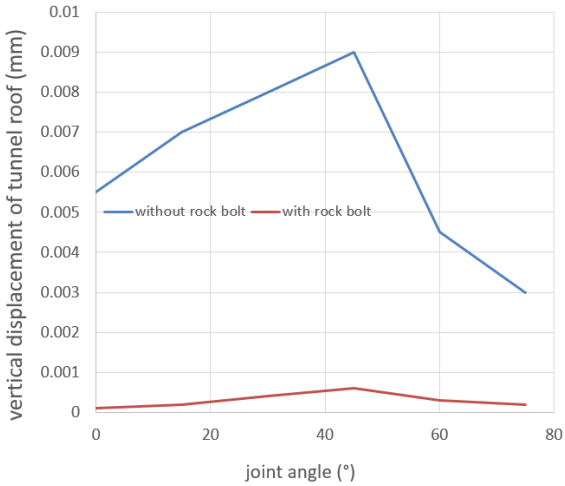

Figure 8. Effect of joint angle on the vertical displacement of tunnel roof with and without the presence of rock bolt when the vertical displacement of loading wall was 0.01 mm.

4. Conclusions

In this work, the interaction between the opening space and the neighboring joint with and without the presence of rock bolt was investigated using the PFC2D simulation. For this purpose, firstly, the calibration of PFC was performed using the Brazilian experimental test and the uniaxial compression test. Secondly, a numerical model with the dimension of 100 mm * 100 mm was prepared. A semi-circular tunnel with a radius of 25 mm was situated below the model. A joint with a length of 40 mm was situated above the tunnel. The joint angles related to the horizontal direction were 0˚, 15˚, 30˚, 45˚, 60˚, and 75˚. Totally, 6 various configurations of the tunnel and neighboring joint were prepared. These models were tested with and without the presence of rock bolts by the biaxial test. The results obtained show that:

- In the absence of rock bolt, two tensile wing cracks initiated from the joint tip and propagated diagonally till coalescence from the model boundary. Also several shear bands were initiated in the left and right sides of the tunnel.
- In the presence of rock bolt, several shear bands were initiated in the left and right sides of the tunnel. The wing cracks disappeared from the joint tips in the presence of rock bolts.
- The stress concentration at the tip of the joint without the presence of rock bolt was more than that with the presence of rock bolt.
- The stress concentration at the tip of the joint had a maximum value when the joint angle was 45˚.
- The vertical displacement of the tunnel roof without the presence of rock bolt was more
- than that with the presence of rock bolt.
- The vertical displacement of the tunnel roof had a maximum value when the joint angle was 45˚.
- The author suggests research works on the interaction between non-persistent open/closed joints and tunnels with and without the presence of rock bolts. In this way, it is possible to investigate the effect of joint matching on the failure behavior of both the supported an unsupported tunnels.

References

[1]. Indraratna, B. and Kaiser, P.K. (1990) Analytical model for the design of grouted rock bolts". International Journal for Numerical and Analytical Methods in Geomechanics. 14 (4): 227–251.

[2]. Li, C. and Stillborg, B. (1999) Analytical models for rock bolts. International Journal of Rock Mechanics and Mining Sciences, 36(8):1013–1029.

[3]. Li, C.C. (2017) Principles of rockbolting design. Journal of Rock Mechanics and Geotechnical Engineering, 9(3), pp. 396–414. 2017.

[4]. Zhao, H., Ru, Z. and Zhu, C. (2018) Reliability-based Support Optimization of Rockbolt Reinforcement around Tunnels in Rock Masses. Periodica Polytechnica Civil Engineering. 62 (1): 250–258.

[5]. Oreste, P. (2005) A probabilistic design approach for tunnel supports. Computers and Geotechnics, 32(7): 520–534.

[6]. Sharan, S.K. (2005) Exact and approximate solutions for displacements around circular openings in elastic-brittle-plastic Hoek-Brown rock. International

Journal of Rock Mechanics and Mining Sciences. 42 (4) 542– 549.

[7]. Sharan, S.K. (2008) Analytical solutions for stresses and displacements around a circular opening in a generalized Hoek-Brown rock. International Journal of Rock Mechanics and Mining Sciences. 45 (1): 78–85.

[8]. Hoek, E. and Brown, E.T. (1980) Underground Excavations in Rock. The Institution of Mining and Metallurgy, London.

[9]. Brown, E.T., Bray, J.W., Ladanyi, B. and Hoek, E. (1983) Ground reponse curves for rock tunnel. Journal of Geotechnical Engineering. 109 (1): 15– 39.

[10]. Cai, Y., Esaki, T. and Jiang, Y. (2004) An analytical model to predict axial loading routed rock bolt for soft rock tunneling. Tunnelling and Underground Space Technology. 19 (6): 607–618.

[11]. Guan, Zh., Jiang, Y., Tanabasi, Y. and Huang, H.W. (2007) Reinforcement mechanics of passive bolts in conventional tunnelling. International Journal of Rock Mechanics and Mining Sciences: 44 (4). pp. 625–636.

[12]. Oreste, P. (2008) Distinct analysis of fully grouted bolts around a circular tunnel considering the congruence of displacements between the bar and the rock. International Journal of Rock Mechanics and Mining Sciences, 45(7): 1052–1067.

[13]. Indraratna, B. and Kaiser, P.K. (1990) Design for grouted rock bolts based on the convergence control method. International Journal of Rock Mechanics and Mining Sciences. 27 (4): 269–281.

[14]. Fahimifar, A. and Soroush, H. (2005) A theoretical approach for analysis of the interaction between grouted rockbolts and rock masses. Tunnelling and Underground Space Technology. 20 (4):333–343.

[15]. Carranza-Torres, C. (2009) Analytical and numerical study of the mechanics of rockbolt reinforcement around tunnels in rock masses. Rock Mechanics and Rock Engineering. 42 (2): 175–228.

[16]. Bobet, A. and Einstein, H.H. (2011) Tunnel reinforcement with rockbolts. Tunnelling and Underground Space Technology. 26 (1):100–123.

[17]. Mollon, G., Daniel, D. and Abdul, H.S. (2009) Probabilistic analysis of circular tunnels in homogeneous soil using response surface methodology. Journal of Geotechnical and Geoenvironmental Engineering. 135 (9):1314–1325.

[18]. Li, H. Z. and Low, B.K. (2010) Reliability analysis of circular tunnel under hydrostatic stress field. Computers and Geotechnics. 37 (1–2): 50–58.

[19]. Lu, Q. and Low, B.K. (2011) Probabilistic analysis of underground rock excavations using response surface method and SORM. Computers and Geotechnics. 38 (8):1008–1021.

[20]. Su, Y.H., Li, X. and Xie, Z.Y. (2011) Probabilistic evaluation for the implicit limitstate function of stability of a highway tunnel in China. Tunnel and Underground Space Technology. 26 (2), pp. 422–434.

[21]. Zhao, H., Ru, Z., Chang, X., Yin, S. and Li, S. (2014) Reliability analysis of tunnel using least square support vector machine. Tunnel and Underground Space Technology, 41:14–23.

[22]. Hoek, E. (1998) Reliability of Hoek-Brown estimates of rock mass properties and their impact on design. International Journal of Rock Mechanics and Mining Sciences. 35 (1): 63–68.

[23]. Zhang, W. and Goh, A.T.C. (2012) Reliability assessment on ultimate and serviceability limit states and determination of critical factor of safety for underground rock caverns. Tunnel and Underground Space Technology, 32: 221–230.

[24]. Itasca Consulting Group Inc, (2008) PFC2D (Particle Flow Code in 2D) Theory and Background," Minneapolis, Minn, USA.

[25]. Potyondy, D.O. and Cundall, P.A. (2004) A bonded-particle model for rock, International Journal of Rock Mechanics and Mining Sciences, Vol. 41, No. 8, pp.1329–1364, 2004.

[26]. Donze, F.V., Richefeu, V. and Magnier S.A. (2009) Advances in discrete element method applied to soil rock and concrete mechanics. Electronic Journal of Geological Engineering 8: 1-44.

رفتار تونل و درز مجاور در حضور پیچ‌سنگ و بدون حضور پیچ‌سنگ تحت بارهای دو محوره، با رویکرد اجزا مجزا

وهاب سرفرازی*

بخش مهندسی معدن، دانشگاه صنعتی همدان، همدان، ایران

ارسال 2020/04/18، پذیرش 2020/05/24

* نویسنده مسئول مکاتبات: sarfarazi@hut.ac.ir

چکیده:

در این تحقیق، با استفاده از کد جریان ذره، اندرکنش بین فضای نیم دایره ای و درزه مجاور با و بدون حضور راک بولت مطالعه شده است. به این منظور، در ابتدا با استفاده از نتایج آزمایشگاهی تک محوره و برزیلی، کالیبراسیون مدل عددی انجام شد. در مرحله دوم، یک مدل عددی با ابعاد 100 mm*100 mm آماده شد. یک فضای نیم دایره ای با شعاع 25 mm در قسمت پایین مدل ایجاد شد. یک درزه با طول 40 mm در بالای تونل ایجاد شد.باز شدگی درزه 2 mm می باشد. زاویه داری درزه نسبت به افق، صفر، 15، 30، 45، 60 و 75 درجه است. بطورکلی 6 نمونه با آرایش متفاوت درزه آماده شد. این مدل ها تحت فشار دو محوره، با و بدون حضور راک بولت، آزمایش شدند. طول راک بولت 50 mm است. مقدار فشار جانبی 2 MPa می باشد. نتایج نشان می دهد که حضور راک بولت، الگوی شکست مدل عددی را تغییر می‌دهد. در غیاب راک بولت، دو ترک کششی از نوک درزه شروع شده و بطور مورب رشد کرده و سرانجام به لبه مدل متصل می‌شود. همچنین، چندین نوار برشی در سمت راست و چپ تونل ایجاد می‌گردد. در حضور راک بولت، فقط چندین نوار برشی در سمت راست و چپ مدل توسعه می‌یابد. مقاومت فشاری با حضور راک بولت بیشتر از مقاومت فشاری بدون حضور راک بولت است. زمانیکه زاویه درزه 45 درجه است، تنش شکست مقدار کمینه دارد.

کلمات کلیدی: کد جریان ذره، تونل، درزه، راک بولت، ترک کششی.